

zations of neutron beams of relatively low density, and on the magnitude of the depolarizing factor  $Q$ .

Referring to Table III, we can see that for each value of  $Q$ , which must be determined approximately by some previous experiment, there will be an optimum value of scattering thickness. On the one hand, the thickness must not be so large as to completely depolarize the beam. On the other hand, the thickness must not be so small

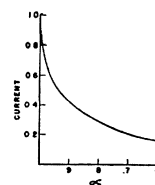


FIG. 7. Reflected current as a function of  $1-2Q$ , second approximation,  $d=10$  (mean free paths).

that a small error in the measurement of the depolarization will result in a large error in  $Q$ .

## A Direct Determination of the Energy of the He<sup>3</sup> Nucleus from the D-D Reaction

HAROLD V. ARGO

*Institute for Nuclear Studies and Department of Physics, University of Chicago, Chicago, Illinois*

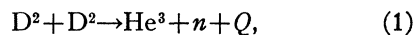
(Received August 2, 1948)

The energy of the He<sup>3</sup> nuclei emitted at 90° to the incident deuteron beam in the D-D reaction has been measured directly by deflecting them through a 90°, 15-cm radius, cylindrical electrostatic analyzer. The He<sup>3</sup> ions were detected by allowing them to eject secondary electrons from the first plate of a 12-element electron multiplier tube. Thus the ions were not required to traverse any foil or window material between the heavy ice target and the point of their detection.

The corrections to be applied to the electrostatic analyzer were experimentally investigated and when applied to the kinetic energies deduced from the observed critical deflecting voltages, give a  $Q$  value of  $3.30 \pm 0.01$  Mev for this reaction.

### INTRODUCTION

THE D-D reaction yielding a neutron and a He<sup>3</sup> nucleus has been studied by observing the recoil He<sup>3</sup> nuclei obtained when a beam of deuterons impinges on a thick target of D<sub>2</sub>O ice. The energy of the He<sup>3</sup> ions emitted at 90° to the incident deuteron beam was measured by deflecting them 90° with an electrostatic analyzer, and the ions were counted with an electron multiplier tube\* of the type developed by J. S. Allen.<sup>1</sup> From the knowledge of the energy of the incident deuteron and the energy of the He<sup>3</sup> nucleus emitted at 90°, one has from conservation of energy and momentum the energy released in the reaction



\* The construction of the electron multiplier tubes for this work was assisted by the Joint Program of the Office of Naval Research and the Atomic Energy Commission.

<sup>1</sup> J. S. Allen, *Phys. Rev.* **55**, 336 (1939); **55**, 966 (1939).

$$Q = E_D + 4E_{He}, \quad (2)$$

where  $Q$  is the energy released,  $E_D$  is the kinetic energy of the incident deuteron, and  $E_{He}$  is the kinetic energy of the He<sup>3</sup> nucleus emitted at 90° in the laboratory system.

### APPARATUS

The deuteron beam was accelerated by a Cockcroft-Walton voltage quadrupling circuit of conventional design employing a low voltage arc source developed by S. K. Allison.<sup>2</sup> Accelerating voltages up to 400 kv could be attained. This voltage was measured by a resistance stack of approximately  $10^{10}$  ohms in series with a sensitive galvanometer. The current through the resistance stack was known to 0.1 percent accuracy, and the resistance to about 0.2 percent. The beam

<sup>2</sup> S. K. Allison, *Rev. Sci. Inst.* **19**, 291 (1948).

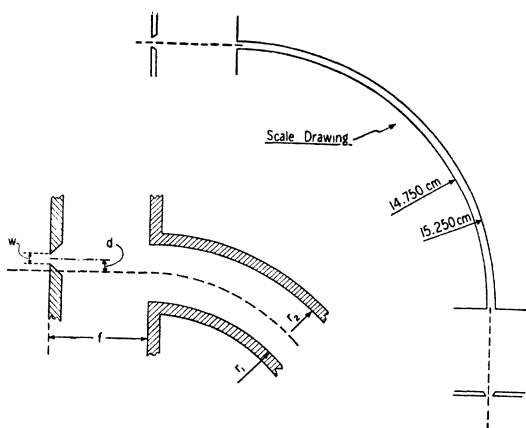


FIG. 1. Schematic illustration of the 15-cm electrostatic analyzer showing the entrance and exit slits.

was accelerated along a 3.0-meter path. At the end of this path an electromagnet was used to deflect the beam horizontally through an angle of  $15^\circ$ . This served to separate the deuteron beam from the other components present. One had the choice of either the atomic deuterium beam or the molecular deuterium beam which, of course, gave deuterons of one-half the accelerating voltage energy. The two beams were of comparable intensity.

The target was placed 100 cm from the deflecting magnet and was insulated electrically from the rest of the system. A  $\frac{1}{4}$ -in. diameter beam stop immediately in front of the target served to limit the beam, and for monitoring purposes a beam current integrator of conventional design measured the beam strength on the target.

The target was a layer of  $D_2O$  ice on a copper slug in good thermal contact with a liquid nitrogen reservoir. The target was laid down continuously during operating by feeding  $D_2O$  vapor into the target chamber by means of a  $\frac{1}{8}$ -in. I.D. tube connecting a small bottle of  $D_2O$  water with the target chamber. This technique was adopted at the suggestion of S. K. Allison to insure having a clean surface layer of  $D_2O$  on the target at all times. Three liquid nitrogen traps were used to reduce the pressure of oil vapor in the system. One trap was placed directly in the target chamber, and the remaining two were placed in the throats of the two six-inch oil diffusion pumps in the large system.

The plane of the target made an angle of  $45^\circ$  with the incident beam and  $45^\circ$  with a vertical line. The entrance slits to the electrostatic analyzer (Fig. 1) were 9.65 cm directly below the target and had a slit width of 3.0 mm.

The electrostatic analyzer used was a new one developed by S. K. Allison<sup>3,4</sup> (Fig. 2). Two cylindrical aluminum plates separated by 0.50 cm deflect the ions through  $90^\circ$ . The average radius of the two plates is 15 cm, and the radii have been held to within  $\pm 0.001$  cm. The plates are supported on a single quartz post 1.5 inches in diameter, placed at their center of curvature, and the diameter of the cylindrical post has been held to a tolerance of  $\pm 0.0001$  inch. Both the position and the width of the entrance and exit slits are adjustable externally.

The entrance and exit slits were placed 5.0 cm from the ends of the deflecting plates of the analyzer. With this arrangement, the fraction of particles collected from a monoenergetic source located at the target is given by

$$(h\Delta r) / \left( 4\pi \left( l_1 + \frac{\pi r}{4} \right) \left( l_1 + l_2 + \frac{\pi r}{2} \right) \right), \quad (3)$$

where  $h$  is the height of the entrance into the

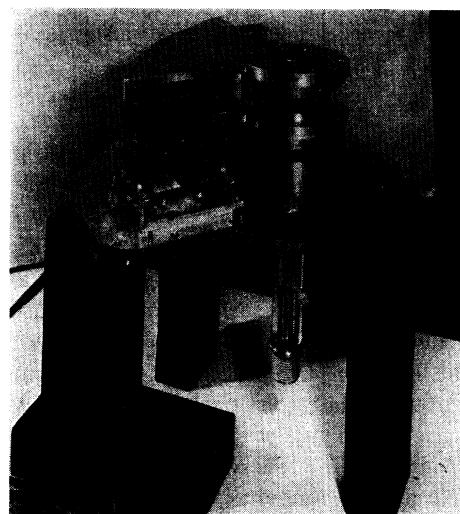


FIG. 2. Photograph of 15-cm electrostatic analyzer with outer shell removed, showing the two concentric cylindrical deflector plates supported by the quartz post. The entrance slit mechanism is in front of the deflector plates.

<sup>3</sup> S. K. Allison and H. V. Argo, Phys. Rev., in press.

<sup>4</sup> Allison, Skaggs, and Smith, Phys. Rev. **54**, 171 (1938).

electron multiplier tube, one inch in this case;  $\Delta r$  is the separation of the two analyzer plates;  $r$  is the mean radius of the two analyzer plates;  $l_1$  is the distance from the target to the entrance end of the plates, 14.65 cm in this case; and  $l_2$  is the distance from the exit end of the plates to the entrance of the electron multiplier tube, which is 12.5 cm. The solid angle factor, as expressed in (3), is calculated to be  $6 \times 10^{-5}$ .

The analyzer does not have perfect resolution,<sup>4</sup> that is, a monoenergetic point source of particles located at the target will not have an infinitely sharp line for its energy spectrum when viewed through the analyzer. Instead, it will have a triangular shaped distribution, as shown in Fig. 3, where  $E$  is the energy of the particles coming from the monoenergetic source, and  $\delta E$  is the half-width, or limit of resolution, of the instrument. For slits of equal width  $w$ ,  $\delta E$  is given by the relationship

$$\delta E/E = w/r, \quad (4)$$

where  $r$  is the mean radius of the analyzer. With a slit width of 3.0 mm and a radius of 15 cm, the limit of resolution for this instrument is 2.0 percent in energy.

Let  $E$  be the kinetic energy, in electron kilovolts, of an ion traversing a circular orbit between the cylindrical electrodes, the orbit being concentric with the plates. Then

$$E = (z |V_2 - V_1|) / (2(\log r_2 - \log r_1)), \quad (5)$$

where

$r_2, r_1$  are the radii of the outer and inner plates, respectively,

$z$  is the number of electronic charges carried by the ion,

$|V_2 - V_1|$  is the numerical value of the difference in potential between the plates, expressed in kilovolts.

Using the dimensions of the present instrument, we obtain

$$E = 15.00 |V_2 - V_1| z. \quad (6)$$

Various authors<sup>5</sup> have discussed the equations of the non-circular orbits and the focal properties of the device. Consider a source emitting mono-

<sup>5</sup> A. L. Hughes and V. Rojansky, Phys. Rev. **34**, 284 (1929); R. Herzog, Zeits. f. Physik **89**, 447 (1934); A. J. Dempster, Phys. Rev. **51**, 67 (1936); F. T. Rogers, Jr., Rev. Sci. Inst. **11**, 19 (1940).

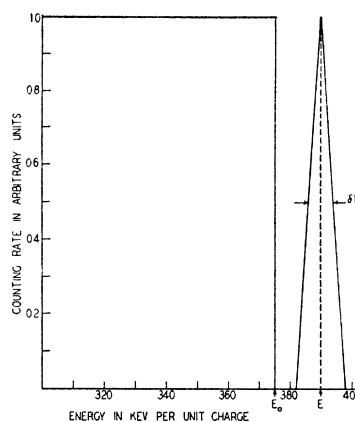


FIG. 3. "Step function" energy distribution of He<sup>3++</sup> nuclei coming from D<sub>2</sub>O ice target as predicted by simple theory.  $E_0$  is the upper energy limit of the spectrum. Also shown is the triangular-shaped energy "window" of the electrostatic analyzer.

energetic ions of kinetic energy  $E_A$ . Let the source be located outside the analyzer, at distance  $f$  from the plane containing the entrance to the cylindrical channel. A divergent bundle of ionic rays, leaving this source and passing through the analyzer, is brought to a focus at a distance  $f'$  from the exit plane, which may be deduced from the two following expressions

$$[(f-g)(f'-g)]^2 = \frac{r_1 + r_2}{2\sqrt{2} \sin(\varphi_m \sqrt{2})}, \quad (7)$$

$$g = (r_1 + r_2 / 2\sqrt{2}) \cot(\varphi_m \sqrt{2}). \quad (8)$$

In these equations,  $\varphi_m$  is the angular length of the path between the plates, in our case,  $\pi/2$ . The important special case  $f = f' = f_0$  is given by

$$f_0 = \frac{r_1 + r_2}{2\sqrt{2}} \frac{1 + \cos(\varphi_m \sqrt{2})}{\sin(\varphi_m \sqrt{2})}. \quad (2)$$

Using the constants of our analyzer, we obtain  $f_0 = 5.29$  cm.

The design of the analyzer was such that the disposition of slits, vacuum walls, etc., that would affect the stray electric field was the same (actually, the two dispositions were mirror images) at the entrance and exit of the cylindrical channel. In these measurements, the distance  $f$  (see Fig. 1) was held at 5.0 cm, close to the value of  $f_0$ , for both entrance and exit slits.

Protons scattered at 90° from a 312-keV beam were used to adjust the instrument. In order to

TABLE I. Test of the correction  $P(\bar{r})$  using deuterons from  $\text{Be}^9(p, d)\text{Be}^8$ ; incident proton energy about 266 kv; slit widths 0.20 cm; half-width at half-maximum of deuterium peaks, 2.5 percent *vs.* 1.3 percent expected from slit widths.

Arrangement	Deflecting kilovolts for maximum counting rate	$E$ from Eq. (5) kev	$P(\bar{r})$	$E_A$ kev
$V_1=0$	$V_2=+39.36$	590.4	+19.7	610.1
$V_2=0$	$V_1=-42.29$	634.4	-21.2	613.2

obtain protons homogeneous in energy, the primary beam was scattered from a very thin film of gold, which had been evaporated onto the polished surface of a beryllium button. The energy spectrum of the scattered protons shows a sharp, high peak from the gold at 312(196/198) kev, with a low, continuous distribution from the underlying beryllium having an upper energy limit slightly below 312(8/10) kev. Such scattered spectra are further discussed in another paper from this laboratory.<sup>6</sup>

Referring to Fig. 1, both slits were set with the width  $w$  at 0.05 cm, and various values of  $d$  were tried, keeping  $d$  the same for the entrance and exit slits, until a position was found in which the counting rate for protons scattered through the device was a maximum. In order to find this position, it was necessary, at each value of  $d$  which was tried, to

- (a) maximize the counting rate as a function of deflecting kilovolts,
- (b) maximize the counting rate as a function of target position.

Operation (a) is called for because of the following considerations. The effective radius  $\bar{r}$ , at which the narrow pencil of rays defined by the two slits passes through the cylindrical channel, is a function of the  $d$  of the slits. In order to cause the central ray in the pencil to traverse this orbit, the deflecting voltage must have such a value that  $E$ , calculated from Eq. (5), is given by

$$E = E_A + P(\bar{r}), \quad (10)$$

where  $P(\bar{r})$  is the gain in energy resulting from the action of the electric field on the ions in passing from the grounded target to a point between the plates of the analyzer at distance  $\bar{r}$  from the axis. Thus the deflecting voltage required to maximize the ion beam is a function of  $d$ .

<sup>6</sup> H. A. Wilcox, Phys. Rev. (to be published).

Operation (b) consisted in moving the target in order to be certain that any trend in the maxima from operation (a) was not due to inhomogeneities in the numbers of protons scattered from the various target areas coming in line with the changing slit positions.

In measuring the  $\text{He}^3$  ions, the centers of the slits were left in the positions located as above; it was, however, necessary to open the slits to a width of 0.3 cm in order to obtain sufficient counting rates. With such an adjustment, it seems clear that the effective radius  $\bar{r} = \frac{1}{2}(r_1 + r_2)$ , and that the value of  $P(\bar{r})$  is  $\frac{1}{2}z(V_1 + V_2)$ .\*\* Since the object of the experiments is to determine  $E_A$ , not  $E$ , it is necessary to apply the "correction"  $P(\bar{r})$ .

The following experiment was performed to test the validity of this correction. A thin target of metallic beryllium evaporated onto polished nickel was bombarded by protons, and the deuteron from the reaction  $\text{Be}^9(p, d)\text{Be}^8$  were deflected through the analyzer.<sup>7</sup> Two different arrangements of  $V_1$  and  $V_2$  were used, and it was ascertained that the correction produced the same value  $E_A$  from both. The data are given in Table I. It is seen that the application of the correction brings the two values together to within 0.5 percent.

The data of the experiments on  $\text{He}^3$  ions were taken with the outer plate of the analyzer at ground potential and the inner plate supplied with a negative high potential.

The high voltage source for the electrostatic analyzer consisted of a 540-cycle generator with a simple half-wave rectifier having a 0.1-mf capacitor, and giving a continuously variable output up to 50 kv. The voltage was measured by means of a wire-wound resistance stack of 20(10)<sup>6</sup> ohms at  $\pm 0.1$  percent, and a 1.5-ma meter calibrated to better than 0.1 percent accuracy. An electrostatic voltmeter was used as a check.

After passing through the electrostatic analyzer the ions were detected by a twelve-electrode electron multiplier tube in the manner already described in detail by L. del Rosario.<sup>7</sup>

\*\* Using this value of the mean potential at the arithmetic mean radius is an obvious, but legitimate, approximation.

<sup>7</sup> See L. del Rosario, Phys. Rev. **74**, 304 (1948).

In brief, the impulse from the collecting electrode of the multiplier tube was fed into a cathode follower and preamplifier of unit gain, and thence into a pulse amplifier, discriminator, and scaler. The discriminator bias was set to accept a minimum pulse height of 0.010 volt from the multiplier tube. The pulse amplifier had a gain of approximately 500.

#### THEORY OF THICK TARGET YIELD

Since the He<sup>3</sup> ions coming from the thick target at 90° are not monoenergetic, one observes an energy spectrum. Some analysis is necessary to determine the energy of the nascent He<sup>3</sup> ions from this spectrum. Those He<sup>3</sup> ions produced deep in the target are due to deuterons which have been slowed down by their passage through the outer layers of D<sub>2</sub>O ice. The He<sup>3</sup> ions will be degraded in energy in passing back out through the ice. Thus the nascent energy will be intimately related to the front edge of the energy spectrum.

The slowing down of low energy He<sup>4</sup> and D<sup>2</sup> ions while passing through gold foils has been measured in this laboratory by H. A. Wilcox.<sup>6</sup> Assuming that the molecular stopping power is the sum of the atomic stopping powers, and that the relative atomic stopping powers as given by Cork<sup>8</sup> hold for these low energies, one can use the results of Wilcox to get the slowing down of D<sup>2</sup> and He<sup>4</sup> ions in D<sub>2</sub>O ice. Assuming that two isotopic ions of the same velocity have very nearly the same rate of energy loss, one can then get the rate of energy loss of He<sup>3</sup> in D<sub>2</sub>O ice. Assuming a *Q* value for this reaction of 3.31 mev, after T. W. Bonner,<sup>9</sup> and an incident energy of 329 kev for the deuterons, one has for the nascent energy of the He<sup>3</sup> ions

$$E_{\text{He}^3} = \frac{1}{4}(Q - E_D) = 745 \text{ kev.} \quad (11)$$

From Wilcox's data one gets for the rate of energy loss of D<sup>2</sup> ions of 329-kev energy passing through D<sub>2</sub>O ice

$$dE/d\tau \sim 270 \text{ kev/mg/cm}^2,$$

and for He<sup>3</sup> ions of 745-kev energy passing

TABLE II. Estimated energies *vs.* depth in target for emergent He<sup>3</sup> ions.

$\tau$ mg/cm <sup>2</sup> traversed to point of creation of He <sup>3</sup>	Deuteron energy in kev at point where He <sup>3</sup> originates	Energy in Mev of nascent He <sup>3</sup>	Energy in Mev of He <sup>3</sup> emerging from target
0	329	0.745	0.745
0.00733	327	0.745 <sub>75</sub>	0.738 <sub>8</sub>
0.0146	325	0.746 <sub>25</sub>	0.731 <sub>8</sub>
0.0220	323	0.746 <sub>75</sub>	0.725 <sub>0</sub>
0.0293	321	0.747 <sub>25</sub>	0.718 <sub>2</sub>
0.0366	319	0.747 <sub>75</sub>	0.711 <sub>5</sub>

through D<sub>2</sub>O ice

$$dE/d\tau \sim 990 \text{ kev/mg/cm}^2,$$

where  $\tau$  is the path length in mg/cm<sup>2</sup>. These loss rates are reasonably constant in the neighborhood of these energies. Thus one can easily find the energy of the deuterons as a function of the path length they have traversed in D<sub>2</sub>O ice. From formula (11) above, one then finds the energy of the nascent He<sup>3</sup> nuclei as a function of the depth in the target at which they were produced. In the energy range which interests us, the energy of the deuteron is a linear function of the amount of material it has traversed, and since the energy of the nascent He<sup>3</sup> nucleus is a linear function of the energy of the deuteron producing it, the curve of energy of nascent He<sup>3</sup> *versus* the point of origin in the target will be a straight line for a considerable range of energy below the upper limit. Table II gives the above argument in a numerical form.

Bennett, Mandeville, and Richards<sup>10</sup> have measured the angular distribution of the D<sup>2</sup>(*d, n*)He<sup>3</sup> reaction in the energy range from 0.5 to 1.8 Mev, using a thin target of D<sub>2</sub> gas. Extrapolating their data to 0.330 Mev and calculating the yield of He<sup>3</sup> to be expected at 90° in the laboratory system, one finds that a 3 per cent decrease in the incident deuteron energy will decrease the yield by approximately 0.5 per cent. As a first approximation we assume that the yield of He<sup>3</sup> in the ice target is independent of the position within the target, at least over the range of interest. Therefore, since the rate of energy loss of He<sup>3</sup> ions in D<sub>2</sub>O ice is a constant in this energy region, one gets in first approximation that the

<sup>8</sup> J. M. Cork, *Radioactivity and Nuclear Physics* (Edwards Brothers, Inc., Ann Arbor, Michigan, 1946), p. 63.

<sup>9</sup> T. W. Bonner, *Phys. Rev.* **59**, 237 (1941).

<sup>10</sup> Bennett, Mandeville, and Richards, *Phys. Rev.* **69**, 418 (1946).

TABLE III. Results.

$E_D$	$E_{He}$ (cf. $E_A$ in Eq. (10))	$Q$ (cf. Eq. (2))	$\Delta^*$	Weight
329 kev	741.5 kev	3.295 Mev	0.007 Mev	10
329	744.0	3.305	0.003	10
329	747.3	3.318	0.016	10
165.5	780.6	3.288	0.014	10
329	745.3	3.310	0.008	3
329	744.6	3.307	0.005	3

\*  $\Delta$  is the deviation from the mean.

emergent  $He^3$  ions are uniformly distributed in energy over a sufficiently wide energy range to warrant treating the energy spectrum as a "step function."

The observed spectrum will be this "step function" as seen through the electrostatic analyzer, which has, effectively, a triangular shaped energy window of 2.0 percent half-width in energy. In Fig. 3,  $\delta E = 0.02E$ .  $E_0$  is the energy of the front edge of the step function, and  $E$  is the energy the analyzer is set to transmit. The ordinate represents the number of ions coming from the target at  $90^\circ$ . As the "window" of the analyzer is moved downward along the energy scale, the number of ions getting through the analyzer is proportional to the area of the triangular window that is overlapped by the step function energy spectrum. This analysis is readily carried out, giving as the observed energy spectrum the curve in Fig. 4.  $E_0$ , the upper limit of the energy distribution of the  $He^3$  nuclei, occurs at 51 percent of the peak counting rate.

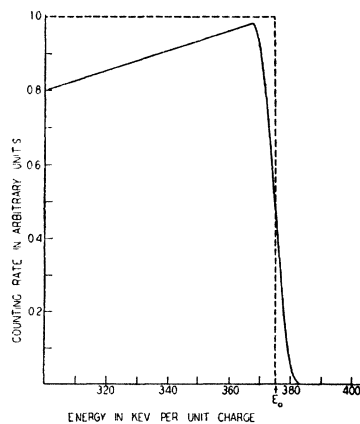


FIG. 4. The energy spectrum of Fig. 3 as observed through the electrostatic analyzer with a slit width of 3.0 mm. The dashed line is the assumed distribution and the solid line the observed distribution according to theory.

The observed curves are slightly more peaked, but have the same slope on the front edge as predicted by the above arguments. In the approximations which resulted in the step function yield from the target, the scattering of deuterons from the incident beam was neglected, as was the scattering of the  $He^3$  nuclei from the emergent beam. The yield of the D-D reaction at  $90^\circ$  is not constant with energy as assumed, but drops off slightly as the energy decreases. In addition, contamination by oil and carbon of the  $D_2O$  layers below the surface layer has been ignored. All of these factors would tend to make the energy spectrum from the target have a more rapid drop off behind the front edge. A calculation using a "saw tooth" function was made, giving Fig. 5 as the predicted observable energy spectrum. The slope of the front edge remains essentially unchanged, while the peak intensity is reduced from 98 percent to 96 percent.  $E_0$  occurs at 52 percent of the peak counting rate.

As the front of the observed and predicted curves is relatively steep,  $E_0$  is well defined. After a comparison of the theoretical with the experimental curves,  $E_0$  was chosen to be that energy corresponding to 52.5 percent of the peak counting rate.

## RESULTS

Figure 6 shows a curve of the type obtainable with this arrangement. This particular curve is of interest because it shows both the  $He^{3++}$  and

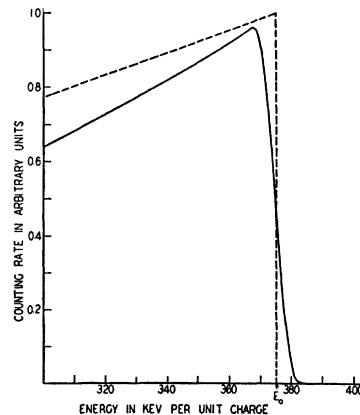


FIG. 5. A "saw tooth" energy distribution of  $He^{3++}$  nuclei coming from thick  $D_2O$  ice target as observed through the electrostatic analyzer with a slit width of 3.0 mm. The dashed line is the assumed distribution and the solid line the observed distribution according to theory.

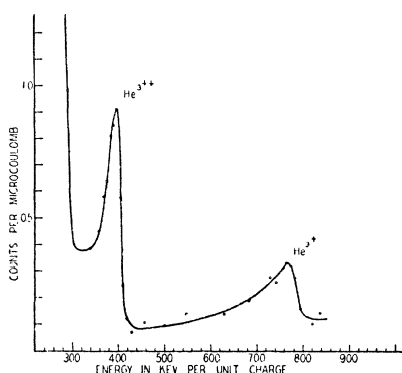


FIG. 6. A curve showing both the  $\text{He}^{3++}$  and  $\text{He}^{3+}$  ions coming from the  $\text{D}_2\text{O}$  ice target. The target was intermediate in thickness.

the  $\text{He}^{3+}$  peaks. The target in this instance was intermediate between a thick and a thin target, and the curve is not suitable for a quantitative measurement of energies.

As an illustration of the operating conditions a typical set of observations is included. For the curve shown in Fig. 7, the accelerating voltage was 329 kv, beam strength on target as measured by the beam current integrator was  $10 \mu\text{a}$ , the current through the electromagnet to obtain a  $15^\circ$  deflection of the deuteron beam was 4.05 amperes, and the peak counting rate for  $\text{He}^{3++}$  ions was approximately 1.6 counts per microcoulomb. The counting periods were monitored at 500 microcoulombs on the target. The circles in the figure are the observed counting rates, while the smooth curve drawn through them is the theoretical one of Fig. 5 scaled to fit these data.

The peaks used for energy determinations in all cases were the  $\text{He}^{3++}$  ions, as these occur at one-half the analyzer voltage required to observe the  $\text{He}^{3+}$  ions, minimizing the natural background of the analyzer.

A total of six curves was obtained. They satisfy the criteria of having the slopes of their front edges agree with the theoretically predicted slope, and having a reasonable scattering of points so that smooth curves could be drawn through them. About an equal number of curves were rejected because of breaks in the front

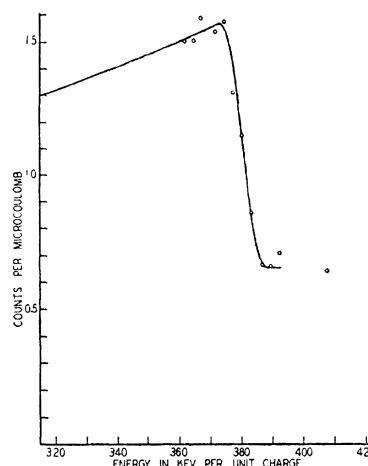


FIG. 7. A typical curve showing the high energy edge of  $\text{He}^{3++}$  particle distribution. The circles are experimental points, and the curve is that to be expected from theory. The abscissae are uncorrected energies per unit charge calculated from Eq. (5).

edges, scattering of points, and too gentle a slope. These troubles were attributed to changes in the target surface during the course of the run. A tabulation of the results appears in Table III. Because of a scattering of the observed points, the last two determinations were given a statistical weight of 3 as compared with a weight of 10 for the others. The resulting value of  $Q$  is  $3.30 \pm 0.01$  Mev.

The best previous measurement of this energy release is due to T. W. Bonner,<sup>9</sup> who has measured the energy carried by the neutron by observing the recoil protons in a cloud chamber. This makes his result dependent upon the range energy relationship for protons. His result is  $Q = 3.31 \pm 0.03$  Mev, which is in agreement with the above value.

#### ACKNOWLEDGMENTS

The author would like to take this opportunity to thank Professor S. K. Allison for suggesting this measurement, and for his advice and assistance during the progress of the work. In addition, he wishes to thank the other members of this laboratory, M. L. Argo, W. R. Arnold, D. Bushnell, and G. W. Farwell for their kind assistance.

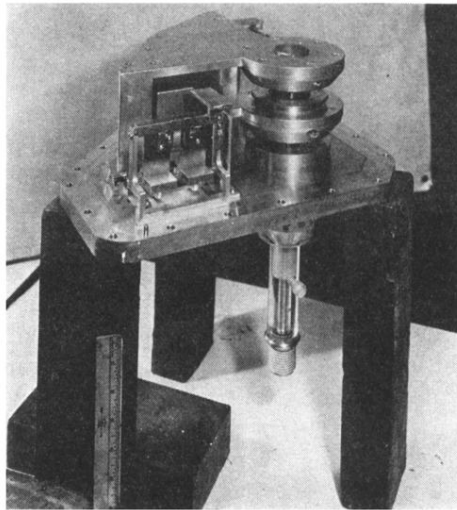


FIG. 2. Photograph of 15-cm electrostatic analyzer with outer shell removed, showing the two concentric cylindrical deflector plates supported by the quartz post. The entrance slit mechanism is in front of the deflector plates.